Available online at www.sciencedirect.com
SCIENCE DIRECT®
Journal of Power Sources 142 (2005) 184–193
JOURNAL OF POWER SOURCES
www.elsevier.com/locate/jpowsour

Modeling and optimization of catalytic partial oxidation methane reforming for fuel cells

A.K. Chaniotis, D. Poulikakos*

Institute of Energy Technology, Laboratory of Thermodynamics in Emerging Technologies, ETH Zentrum, IET, LTNT, Sonneggstrasse 3, CH-8092 Zürich, Switzerland

Received 24 May 2004; received in revised form 5 October 2004; accepted 23 October 2004
Available online 16 December 2004

Abstract

The objective of this paper is the investigation and optimization of a micro-reformer for a fuel cell unit based on catalytic partial oxidation using a systematic numerical study of chemical composition and inflow conditions. The optimization targets hydrogen production from methane. Additionally, the operating temperature, the amount of carbon formation and the methane conversion efficiency are taking into account. The fundamental investigation is first based on simplified reactor models (surface perfectly stirred reactor (SPRS)). A detailed surface chemistry mechanism is adopted in order to capture all the important features of the reforming process. As a consequence, the residence time of the process is taken into account, which means that the products are not necessary in equilibrium. Subsequently, in order to test the validity of the findings from the simplified reactor model, more detailed simulations (involving the Navier–Stokes equations) were performed for the regions of interest. A region where all the targeted operating conditions are satisfied and the yield of hydrogen is around 80% is identified.

Keywords: Catalytic partial oxidation; Methane reforming; Hydrogen production; Micro-reformer

1. Introduction

The interest in production of hydrogen from hydrocarbons has grown significantly in the last decade [1]. Efficient production of hydrogen is an enabling technology, directly related to the fuel cell energy conversion device [2]. Most of the fuel cells involve electrochemical reactions of hydrogen on the anode. The obvious operating scenario of storing the hydrogen and directly supplying it to the fuel cell is suffering from the safety point of view. There are few examples of direct fuel conversion of hydrogen inside the cell, mainly in high temperature fuel cells. As a consequence, fuel processors are considered an important unit in conjunction with the fuel cell converter. Fuel processors are usually described as relatively heavy, bulky, requiring relative high residence times and without practical dynamic response.

The optimal coupling of a fuel-processing unit with the fuel cell is generally considered essential in order to achieve high efficiencies. The reforming can be non-catalytic [3,4] or catalytic [5–7]. The latter can achieve higher conversions, with lower operating temperatures and drastically smaller residence times compared to its non-catalytic counterpart. The small residence time is an essential parameter in order to reduce the size of the reformer and becomes necessary for portable fuel cell applications. The catalytic conversion of fuels to hydrogen can be carried out by three major techniques: the steam reforming, the partial oxidation and the auto-thermal reforming. Steam reforming is the most common method for producing hydrogen and it is based on the reaction of fuel with water. The main steam reforming reactions are strongly endothermic. The heat required for the reaction is supplied from an external source and the reactor

* Corresponding author. Tel.: +41 1 63 22 435; fax: +41 1 63 21 176.
E-mail addresses: andreas.chaniotis@ethz.ch (A.K. Chaniotis), dimos.poulikakos@ethz.ch (D. Poulikakos).

0378-7753/$ – see front matter © 2004 Elsevier B.V. All rights reserved.
doi:10.1016/j.jpowsour.2004.10.018

design is usually limited by heat transfer [8]. The partial oxidation method relies on the reaction of the fuel with air in order to produce carbon oxides and hydrogen. The main reaction is exothermic leading to high temperatures. The auto-thermal reformers combine the thermal effects of partial oxidation and steam reforming. Fuel, air and steam are fed to the reactor, the steam reforming reactions absorb the heat generated by partial oxidation and decrease the operating temperature. Together with the autothermal reaction the shift-reaction and the total oxidation occur.

In the present work, we present a systematic numerical investigation of the catalytic reforming of methane with partial oxidation. Rhodium (Rh) catalysts are preferred to reform natural gas [6,9–11] which leads to high fuel conversion and selectivities. The main advantages of catalytic partial oxidation are its exothermic and the kinetically controlled reactions. The exothermic character of partial oxidation has as consequence low demand of energy and the kinetically controlled reactions lead to short contact times. However, the major challenge is that the partial oxidation path is competing with the total oxidation. Hence, the reforming based on partial oxidation is considered to have lower efficiency compared to steam and auto-thermal reforming, but it does not require any amount of water which would add complexity to the system in particular for portable applications.

There are several approaches in modeling catalytic reaction systems [12,13]. A simple 1D approach is based on plug-flow reactor models. The plug-flow has zero gradients in the radial direction and the surface reactions are applied to the entire section. These models are based on the derivation of balances for conservation of mass, energy and momentum over finite differential slices in the flow direction. The transport along the transverse direction and axial diffusion are neglected [14]. In order to investigate the spatial profiles with more detail, multidimensional models are required. After the work of Young and Finlayson [15] there are several 2D simulations published [13,16–19] based on the Navier–Stokes equations. The boundary layer model [20,21] is often used, where the assumption of negligible axial diffusion simplifies the solution algorithm and the computational cost. A notable comparison of the boundary layer formulation and the complete Navier–Stokes equation model using detailed surface chemistry kinetics is presented in [19] where, surprisingly, it was observed that the sophisticated chemistry models are the driving mechanism and not the exact description of all flow features of the process. Significant effort aims at the investigation of chemical kinetics with respect to the homogeneous and heterogeneous contributions in order to understand the relative paths and investigate the applicability of the chemical mechanisms [22–25]. Among the multidimensional models 3D simulations of monolith channels [26,27] and full-scale monolith simulations based on sub-grid scale approach [27] have appeared but they are rare. A complex detailed model is always necessary in order to prove the validity and usefulness of simpler models.

The main goal of the present study is to define operating conditions for a microscale reactor, which lead to efficient hydrogen production from methane reforming with partial oxidation. In order to optimize the reactor we first use simplified low-dimensional models such as the surface perfectly stirred reactor (SPSR). To ensure the validity of the findings we also perform simulations using more comprehensive models involving the Navier–Stokes equations. Using this approach we achieve optimization of the reactor with respect to the chemical composition and inflow conditions in a rigorous manner, while the computational cost is small.

2. Single channel reactor

In order to achieve high surface to volume ratio with reasonable pressure drop, which is desirable in catalytic reactions, a usual reactor configuration are the monoliths [28]. Monoliths are arrays of regularly shaped channels (Fig. 1). In our modeling we focused on a single monolith reactor configuration. The single channel can be considered as a part of a monolith structure and from the modeling point of view only one channel needs to be investigated, assuming that symmetry holds for the inlet conditions. The single channel reactor is a cylindrical tube with diameter 1 mm and length 10 mm. The diameter of the channel was chosen to be 1 mm because it is comparable to sizes proposed in many microscale reactors [28,29]. The tube inner surface is covered by Rh with surface site density 2.7×10^9 mol cm^{-2} [26,30]. The inlet mixture is methane/air. Based on the partial oxidation of methane

$$CH_4 + \tfrac{1}{2}O_2 \rightarrow CO + 2H_2 \quad (1)$$

we can define the equivalence ratio ϕ as the ratio of the actual fuel/oxygen ratio to the stoichiometric fuel/oxygen ratio (Eq. (2)). Stoichiometric reaction occurs when all the oxygen and methane is consumed in the reaction. If the equivalence

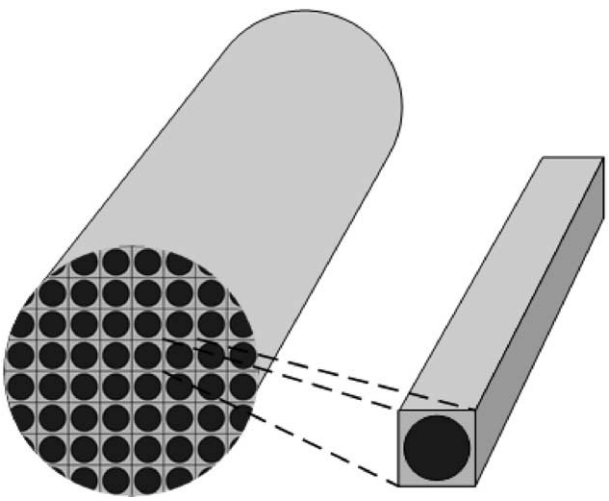

Fig. 1. Sketch of a monolith and enlarged view of an individual channel.

ratio ϕ is equal to unity, the combustion is stoichiometric. If it is less than unity, the combustion is lean with excess oxygen, and if it is more than unity, the combustion is rich with excess of methane.

$$\phi \equiv \frac{(\text{mass of } CH_4)/(\text{mass of } O_2)}{((\text{mass of } CH_4)/(\text{mass of } O_2))_{\text{stoichiometric}}} \quad (2)$$

The equivalence ratio ϕ is used in order to define the inlet chemical composition of the reactor.

The channel wall is assumed to be thermally thin and axial conduction is neglected. We note that axial conduction and radiation may have some impact on the performance of the reactor and will be considered in future investigations. All the computations are performed with adiabatic walls at atmospheric pressure. In order to investigate the performance of the reformer we focus on the production of hydrogen. For this reason we define the hydrogen yield as

$$\text{Yield}_{H_2} \equiv \frac{\text{mass of } H_2}{\text{theoretically maximum mass of } H_2} \quad (3)$$

where the "theoretical maximum" is calculated only from the partial oxidation reaction.

The current work focuses on the effect of composition, inlet velocity and inlet temperature (the reactor operating conditions) on the performance of the reactor.

3. Numerical models

Although monolith catalysts are currently commercial products [28], there are still open questions concerning their activity and durability during extreme thermal conditions. A proper design of reforming requires operation at specific temperatures and conversion rates. Next to fundamental issues of material science, modeling can be extremely useful in sizing the reactor, investigating its behavior in operation, and predicting the dynamic effect of operating conditions. Temperature, fuel and soot distributions in the channels are needed information that determines the behavior of the monolith. The high temperature along the channel can deactivate and damage the catalyst and high soot formation on the catalyst can reduce the efficiency of the reactor. Experimental investigations are expensive, while theoretical models in which mass, momentum and heat transfer are solved, need sufficient physicochemical data.

Our modeling strategy is based on some general assumptions. The Reynolds number based on channel diameter and inflow conditions is smaller than 500 and the flow filed is considered laminar. The steady state results are used for comparison [19]. Only one channel of the monolith is simulated and the walls of the channel are considered adiabatic [30]. The conductivity of the walls and the heat flux by radiation are neglected [13,17,19]. An order of magnitude analysis showed that the heat conducted axially along the channel wall for ceramic materials is indeed negligible (approximately 0.05%) compared to the released energy of reaction. The gas mixture is assumed to follow the ideal gas law and the thermodynamic and transport properties depend on temperature [31–33]. A detailed surface reaction mechanism of methane on rhodium is used for all the simulations [26,30]. This heterogeneous mechanism takes into account intermediate reaction steps (38 elementary surface reactions) and species (7 gas phase and 12 site species) and can describe precisely partial and full oxidation of methane on rhodium. The homogeneous gas phase reactions are neglected [17,19,29] since the residence time of the heterogeneous reactions is smaller. It is also reported [30] that for moderate temperature the effect of gas phase chemistry is not significant.

3.1. Surface perfectly stirred reactor model

Perfectly stirred reactor models have been used extensively for many years in simulations of reacting systems for a variety of applications. Chemical vapor deposition systems can be modeled using perfectly stirred reactor models that include a detailed surface reaction mechanism [34]. Many other catalytic and materials applications have been modeled using the SPSR [35,36]. The basic assumption of the SPSR is that mixing of the reactants is so complete that the conversion of reactants to products is determined by the chemical reaction rates rather than the diffusion, convection, or other transport processes [34]. In our simulations we define the inlet temperature, velocity and mixture, and we monitor the species fractions and temperature at the outlet of the reactor. Since the residence times of catalytic reactions is very small, and the flow residence time of the channel we simulate is also small, we consider that the outlet composition is not necessary in thermodynamic equilibrium but agrees with the thermodynamic equilibrium in the limit of long residence times. For this reason, an optimization based on SPSR can provide more information compared to optimization based only on thermodynamic analysis using Gibbs free energy minimization [37–41] or, based on the atomic balance approach [42]. The modeling we present here is feasible only for fuels and catalysts for which we already have a reaction mechanism.

3.2. Navier–Stokes equation model

In order to verify the results from the SPSR we also perform detailed calculations based on the Navier–Stokes equations. The simulations are carried out using the CFD-ACE+ commercial multi-physics computational application developed by ESI CFD in Huntsville, Al, USA. The CFD-ACE+ software is capable of solving the governing system of equations of mass, momentum, energy and species coupled with boundary condition for surface reactions. More details concerning the numerical techniques required to solve the system of equations are beyond the scope of this article, and may found elsewhere [43–45]. Validation of the CFD-ACE software is presented in [27] where numerical catalytic combustion results of a hydrogen-methane-air mixture on a platinum coated monolith are compared to experimental results [46].

The fundamental set of equations has the general form [31]

$$\frac{\partial \rho}{\partial t} + \nabla(\rho \mathbf{U}) = 0 \tag{4}$$

$$\frac{\partial \rho \mathbf{U}}{\partial t} + \nabla(\rho \mathbf{U}\mathbf{U}) = -\nabla p + \nabla \boldsymbol{\tau} + \mathbf{B} \tag{5}$$

$$\frac{\partial \rho h}{\partial t} + \nabla(\rho \mathbf{U} h) = -\nabla \mathbf{q} + \boldsymbol{\tau} : \nabla \mathbf{U} + \frac{\mathrm{d}p}{\mathrm{d}t} \tag{6}$$

$$\frac{\partial \rho Y_i}{\partial t} + \nabla(\rho U Y_i) = -\nabla \mathbf{J}_i + \dot{\omega}_i \tag{7}$$

$$p = \rho R T \sum_{i=1}^{N_{\mathrm{Gas}}} \frac{Y_i}{W_i} \tag{8}$$

where ρ is the fluid density, $\mathbf{U}$ is the velocity vector, p is the pressure, $\boldsymbol{\tau}$ is the shear stress tensor, $\mathbf{B}$ is the body force vector, h is the enthalpy, $\mathbf{q}$ is the heat flux, i is the gas phase species index, Y_i is the mass fraction of the ith species, $\mathbf{J}_i$ is the species diffusive flux,ω_i is the production rate of the ith species, T is the bulk temperature and W_i the molecular weight of the ith species. The heat flux $\mathbf{q}$ is written as

$$\mathbf{q} = -k\nabla T + \mathbf{q}_R + \sum_{i=1}^{N_{\mathrm{Gas}}} \mathbf{J}_i h_i \tag{9}$$

where k is the conductivity, $\mathbf{q}_R$ is the heat flux due to radiation and the last term is the heat flux due to species diffusion. N_{Gas} is the total number of gas species, $\mathbf{J}_i$ is the mass diffusion fluxes of the ith species and h_i the enthalpy of the ith species. The mass diffusion species is written in the classical Fickian form [47] as:

$$\mathbf{J}_i = -\rho D_i \nabla Y_i - D_i^{\mathrm{T}} \frac{\nabla T}{T} \tag{10}$$

where D_i and D_i^{T} are the mass and thermal mixture average diffusion coefficients [33] where for the present simulations we do not include any corrections [48], which is also the case in most numerical simulations of monolith channels [19,49]. The influence of species on thermal transport (Dufour effect) is of minor importance [50]. Radiation is also neglected, but we recognize that may have some impact on the performance of the reactor and will be considered in future investigations.

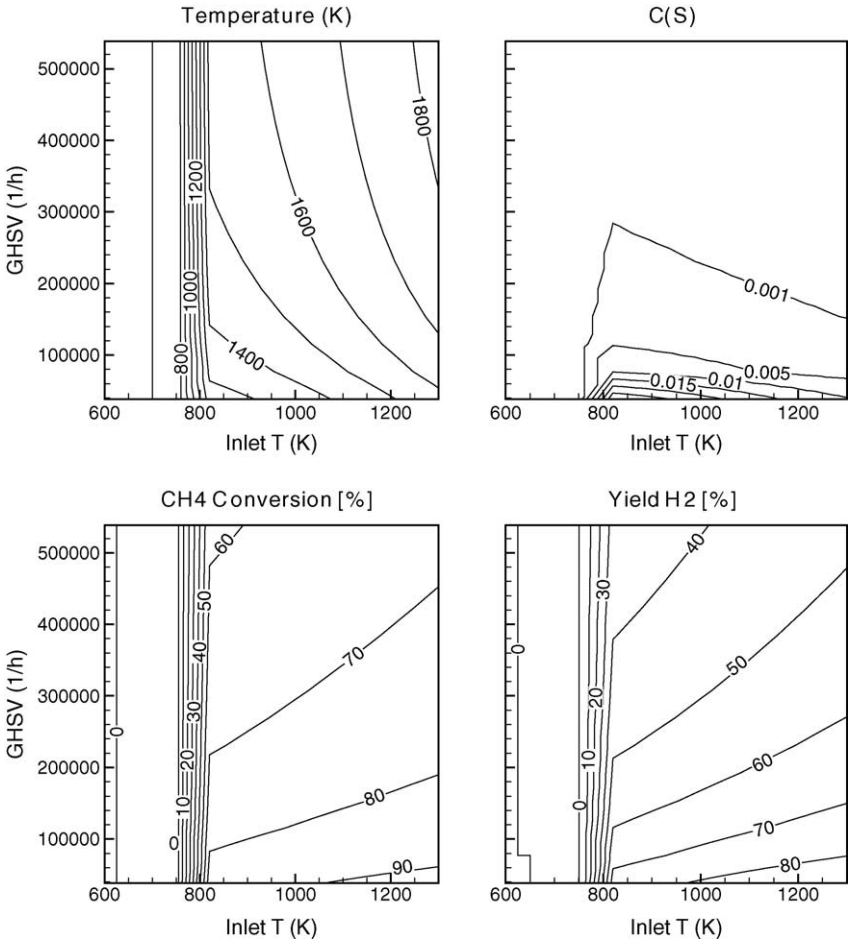

Fig. 2. Reactor temperature, carbon soot, methane conversion and hydrogen yield (calculated from the SPSR model using only surface reactions) as a function of inlet temperature and space velocity for the equivalence ratio of $\phi = 1.0$.

The chemical reactions on the catalytic surface lead to the following boundary condition [51]

$$\mathbf{n} \cdot [\rho Y_i \mathbf{U}_S + \mathbf{J}_i] = \dot{s}_i W_i \tag{11}$$

where $\mathbf{n}$ is the unit inward pointing vector to the surface, $\mathbf{U}_s$ is the so-called Stefan velocity which occurs when there is a net mass flux between the surface and the gases and $\dot{s}_i$ is the production rate of the ith species due to chemical reaction at the surface. More details concerning the implementation and the solution procedure can be found in [45].

4. Results and discussion

In order to investigate the reformer and optimize the hydrogen production we performed systematic simulations of the specific monolith channel described in Section 2. The chemical composition is described by the equivalence ratio ϕ (Eq. (2)) and the inlet conditions by the inlet temperature and gas hours space velocity (GHSV). (The GHSV is defined as the ratio of the volumetric flow of reactants at standard conditions (25 °C and 1 atm) to the total catalyst volume and has units of inverse time).

$$\mathrm{GHSV} = \left(\frac{\dot{m}_{\mathrm{inlet}}}{\mathrm{Vol}_{\mathrm{catalyst}} \ \rho_{\mathrm{inlet}}} \right)_{\mathrm{ST}} \tag{12}$$

where $\dot{m}_{\mathrm{inlet}}$ is the mass flow rate of the reactants, ρ_{inlet} it the density of the reactants and $\mathrm{Vol}_{\mathrm{catalyst}}$ is the total catalyst volume.Out of the extensive set of cases that have been simulated using the SPSR configuration, the reactor operating temperature, the carbon soot $C(s)$ (surface coverage), the methane conversion and the yield of hydrogen are presented in Fig. 2, as a function of inlet temperature and inlet space velocity for equivalence ration $\phi = 1$. From the map of temperature in Fig. 2 we can identify the ignition region of the mixture. From similar simulations using SPSR for different values of equivalence ratio ϕ we observe that the mixture of methane and air is ignitable for inlet temperatures $T > 780 \pm 20$ K. Increasing the inlet temperature we observe in Fig. 2 that the operating temperature of the reactor increases and at the same time the conversion of methane and the yield of hydrogen also increase.

In Fig. 3 we present the reactor operating temperature, the carbon soot, the methane conversion and the hydrogen

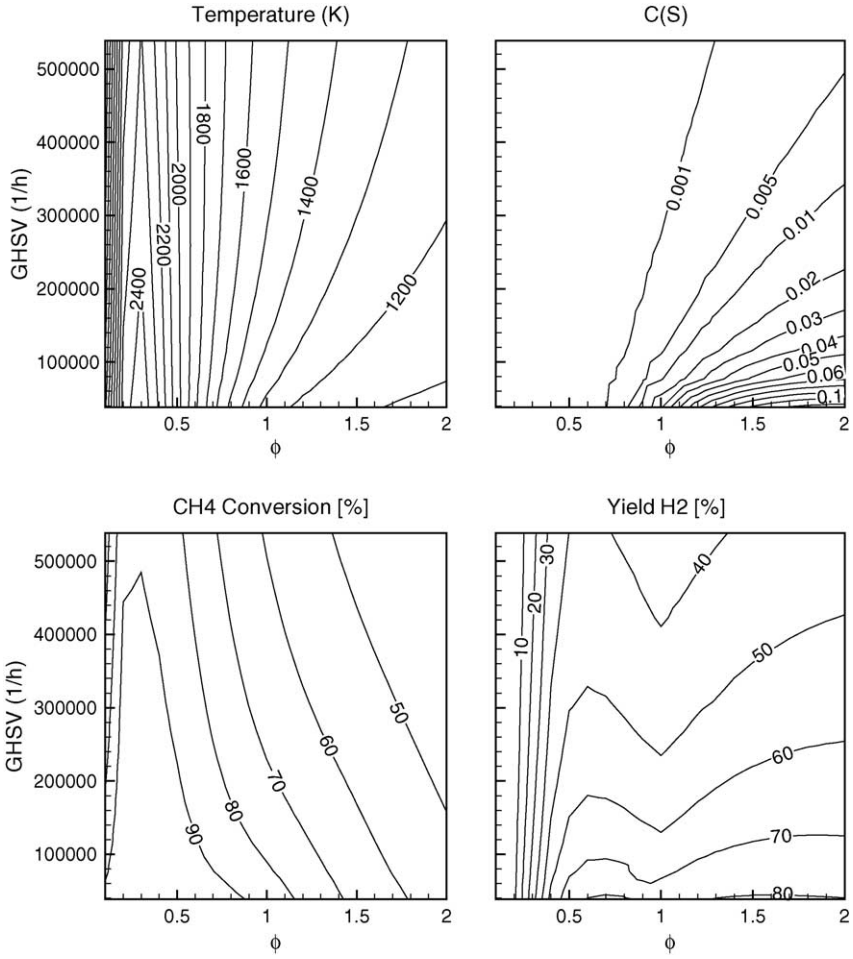

Fig. 3. Reactor temperature, carbon soot, methane conversion and hydrogen yield (calculated from the SPSR model using only surface reactions) as a function of the equivalence ratio ϕ and space velocity for the inlet temperature $T = 850$ K.

yield as functions of the equivalence ratio ϕ and the inlet space velocity for the inlet temperature of $T = 850$ K. From the operating temperature map in Fig. 3 we can identify the high temperature region ($0.2 < \phi < 0.4$) which corresponds to full oxidation of methane and leads to high conversion of methane but low hydrogen yield. The carbon soot increases when the equivalence ratio increases and decreases when the space velocity increases. The hydrogen yield exhibits a non-monotonic dependence on the equivalence ratio. The region ($0.5 < \phi < 1.0$) in Fig. 3 shows an interesting behavior because the hydrogen yield exhibits a local maximum while the operating temperature is relatively low ($T < 1800$ K), and the carbon shoot is also low ($C(s) < 0.01$). The hydrogen yield achieves values approximately 70–80% in the region of equivalence ratio $0.5 < \phi < 1.0$ for low space velocities. This region of equivalence ratio ϕ for low space velocities appears to have at the same time high values of hydrogen yield and appealing operating conditions regarding reactor temperature and carbon shoot production compared to other regions of the map with high yield. The reactor temperature is a quantity related to the lifetime of the catalyst, while the carbon soot is related to the efficiency of the reactor. For the higher inlet temperature $T = 950$ K (Fig. 4) we observe the same qualitative behavior as in Fig. 3. In Fig. 4 we can identify a relative increase in temperature and carbon soot compared to Fig. 3 and the region of equivalence ratio $0.5 < \phi < 1.0$ results in high values of hydrogen yield (≈70%) for low space velocities. For even higher inlet temperatures (not shown here for brevity) we observe an analogous behavior.

In Fig. 5 the reactor operating temperature, the carbon soot the methane conversion and the hydrogen yield are presented as a function of the inlet velocity for the inlet temperature of $T = 875$ K and for five different values of equivalence ratio ϕ in the region of interest ($0.5 < \phi < 1.0$) identified earlier. We can observe that the temperature of the reactor and the methane conversion decrease significantly with increasing the equivalence ratio. For the region of interest, the effect of velocity on the rector temperature is relatively small. The carbon soot is strongly related to the equivalence ratio ϕ (Fig. 5). The hydrogen yield appears to markedly depend on the inlet velocity. Additionally, we observe the local maximum of hydrogen yield in the region $0.6 < \phi < 0.7$ which was also

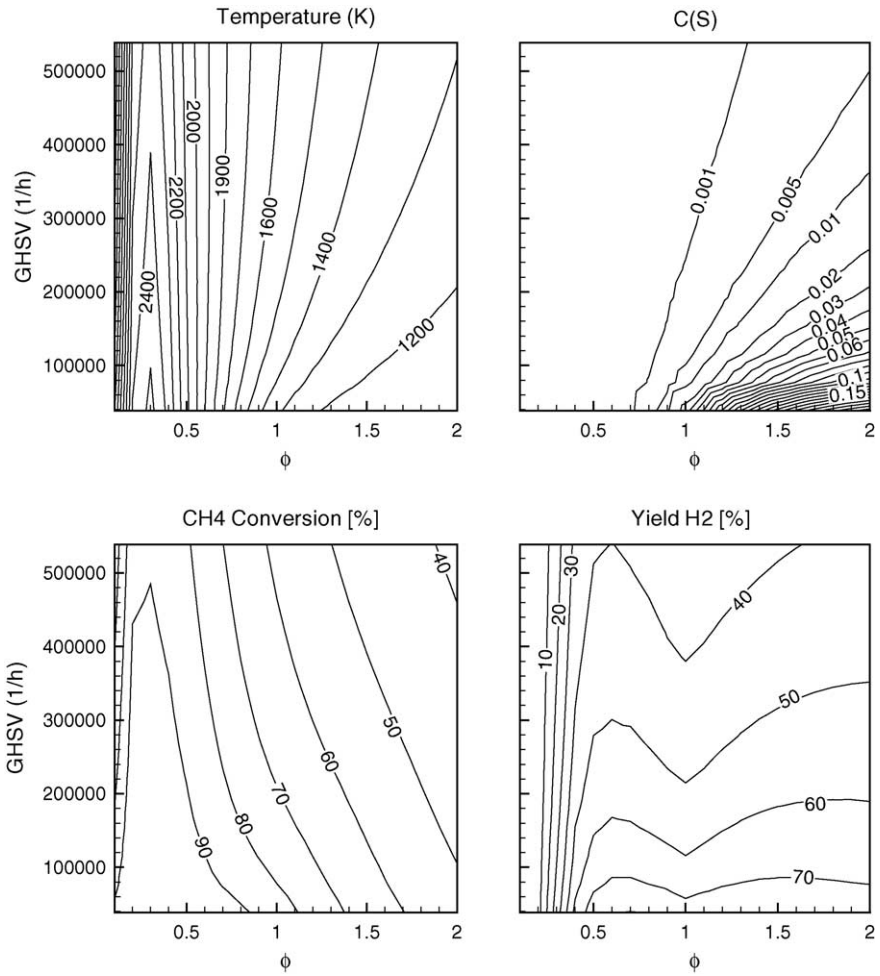

Fig. 4. Reactor temperature, carbon soot, methane conversion and hydrogen yield (calculated from the SPSR model using only surface reactions) as a function of the equivalence ratio ϕ and space velocity for the inlet temperature $T = 950$ K.

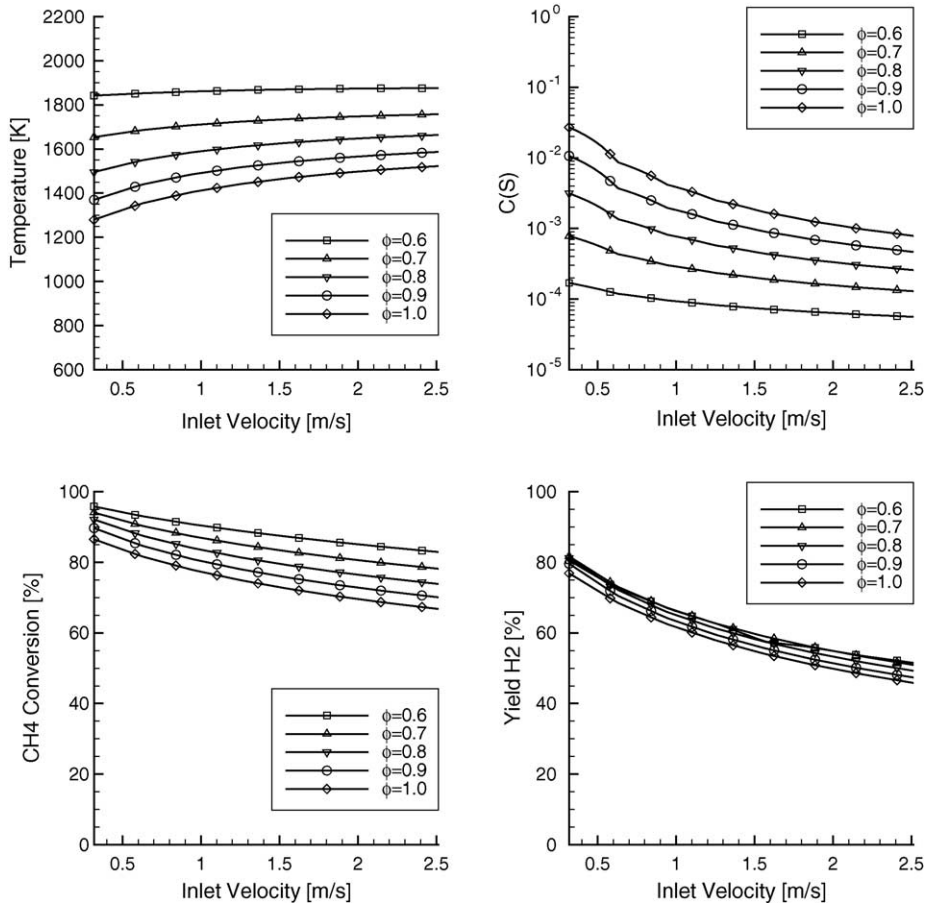

Fig. 5. Reactor temperature, carbon soot, methane conversion and hydrogen yield (calculated from the SPSR model) for different equivalence ratios ϕ using only surface reactions as a function of the inlet velocity for inlet temperature $T = 875$ K.

observed in Fig. 4. In Fig. 5, the graphs of rector temperature, carbon soot methane conversion and yield of hydrogen delineate the counteractive behavior of the quantities of interest. For the production of hydrogen it is better to have low inlet velocities. The effect of inlet velocity is more visible in Fig. 6 where the yield of hydrogen is shown as a function of the equivalence ratio ϕ for different inlet velocities. At the same time, the low inlet velocities lead to higher fractions of carbon soot which can degrade the efficiency of the catalyst (Fig. 5). The low inlet velocities are also advantageous from the mechanical point of view since they lead to a reasonable pressure drop due to the monolith structure [27].

The results presented in Figs. 2–6 are based on simulations using the SPSR configuration. The SPSR configuration has a number of fundamental differences compared to the monolith channel reactor configuration. The SPSR simulations are useful in order to extract qualitative results and conclusions. In order to further quantify and verify the SPSR results, it is necessary to perform more comprehensive multidimensional simulations. For this reason we performed detailed simulations, using the Navier–Stokes solver discussed in Section 3.2, for the region of interest of equivalence ratio $0.6 < \phi < 1.0$ and for low inlet velocities.

In Fig. 7, the numerical results of temperature, carbon soot, methane and hydrogen mass fraction along the channel are shown, using detailed surface reactions mechanism for equivalence ratio $\phi = 0.7$, inlet velocity $U = 1\ \mathrm{m\ s^{-1}}$ and inlet temperature $T = 875$ K. The channel is discretized using a

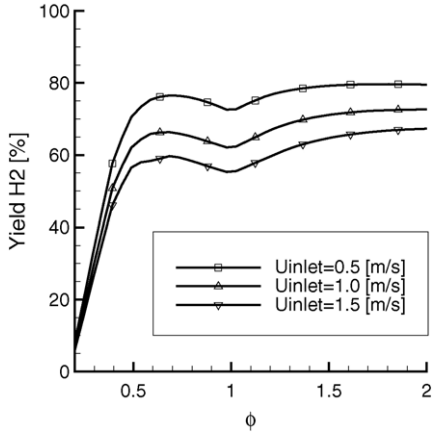

Fig. 6. Hydrogen yield calculated from the SPSR model, for different inlet velocities using only surface reactions as a function of the equivalence ratio ϕ for inlet temperature $T = 875$ K.

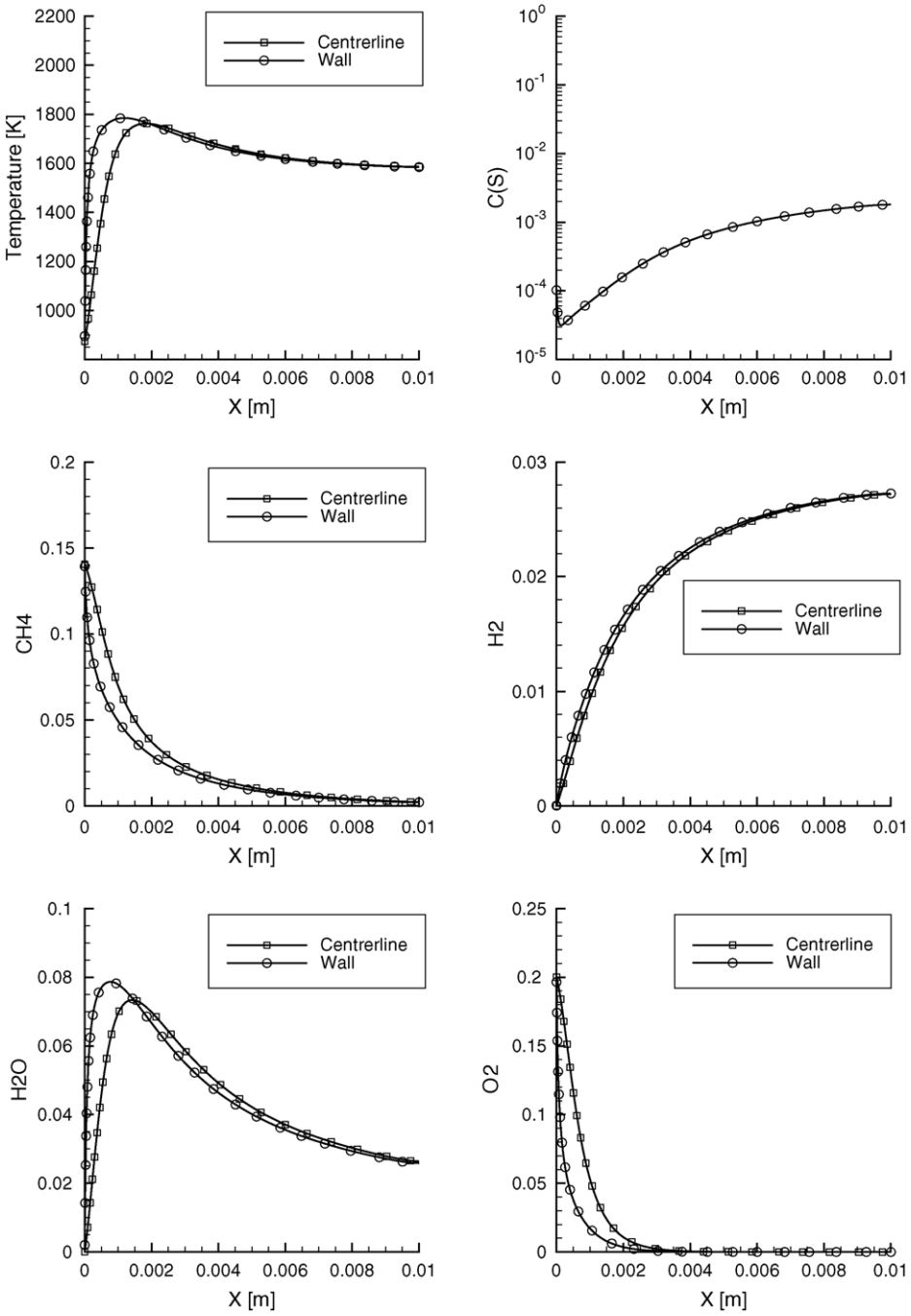

Fig. 7. Temperature, carbon soot, methane, hydrogen, water and oxygen mass fraction along channel, calculated from the Navier–Stokes model using only surface reactions for equivalence ratio $\phi = 0.7$, inlet velocity $U = 1\ \mathrm{m\,s^{-1}}$ and inlet temperature $T = 875\ \mathrm{K}$.

non-uniform mesh having 150 axial elements and 50 radial elements. The nodes are concentrated near the wall and at the beginning of the catalyst. A mesh resolution study confirmed that the grid 150×50 produces fully resolved numerical solutions. From the temperature plot in Fig. 7 we observe that the wall reaches very fast a maximum temperature, which is followed by a significant reduction until the end of the channel. The maximum temperature at the beginning of the channel is due to the full oxidation of methane, which produces significant amount of water. The water in the presence of methane at high temperature subsequently enhances the steam reforming process (Eq. (13)) which produces more hydrogen. The endothermic character of steam reforming leads to the temperature drop until the end of the channel.

$$\mathrm{CH_4 + H_2O \rightarrow CO + 3H_2} \tag{13}$$

In order to determine the effect of the equivalence ratio ϕ for the region $0.6 < \phi < 1.0$ a series of simulations was performed.

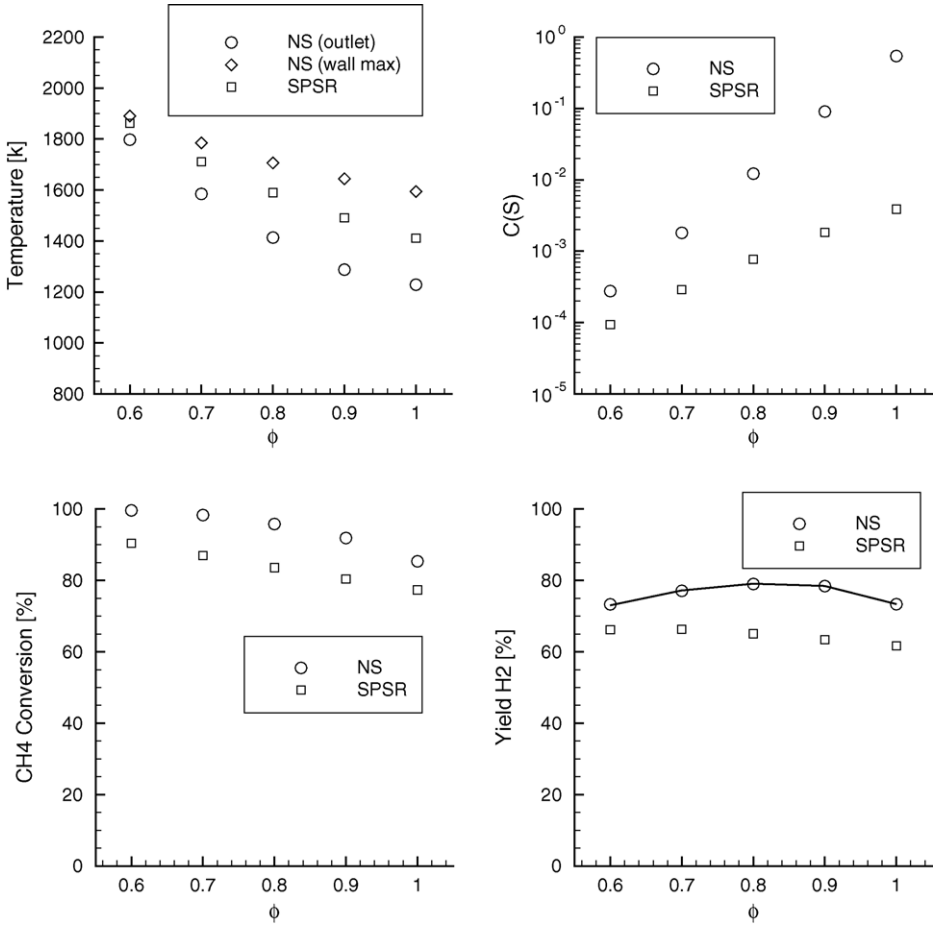

Fig. 8. Temperature, carbon soot, methane conversion and hydrogen yield calculated from the Navier–Stokes and the SPSR model for different equivalence ratios ϕ using only surface reactions. The inlet velocity is $U = 1\,\mathrm{m\,s^{-1}}$ and the inlet temperature is $T = 875\,\mathrm{K}$.

In Fig. 8 we present the results for inlet velocity $U = 1\,\mathrm{m\,s^{-1}}$ and inlet temperature $T = 875\,\mathrm{K}$ where we compare the findings from the two-dimensional Navier–Stokes solver with the SPSR results. The qualitative agreement between the Navier–Stokes model and the SPSR model is indeed good. The SPSR simulations predict all the trends of the dependence of temperature, carbon soot and methane conversion on the equivalence ratio. More important is the comparison of the hydrogen yield. The detailed Navier–Stokes simulation shows high values of hydrogen yield (≈70–80%) for the region of interest $0.6 < \phi < 1.0$. The position of maximum is only slightly shifted and is about 5–10% higher compared to the SPSR prediction, underpinning the usefulness of the latter

5. Conclusions

A systematic analysis has been conducted in order to investigate the process of hydrogen production from methane using partial catalytic oxidation. The analysis focuses on the inlet conditions such as temperature, velocity and chemical composition for a typical monolith configuration. The investigation is first based on the surface perfectly stirred reactor model. In the simulations detailed surface chemistry mechanism is adopted in order to capture all the important features of the reforming process. Regions of efficient hydrogen production are so identified. These regions where further investigated with comprehensive simulations using a Navier–Stokes equations solver and detailed surface chemistry. The predictions of the Navier–Stokes model agree satisfactorily with the SPSR model values of hydrogen yield. The agreement between the simplified model (SPSR) and Navier–Stokes equation model is due to the fact that in both cases the apparently important surface chemistry is modeled in detail and the residence time of the reactor is captured accurately. The finite radial diffusion of the Navier–Stokes model compared to the infinite diffusion of the SPSR seems not be important in our case study, since the residence time in the channel is a multiple of the radial diffusion time.

The hydrogen production is strongly depended on the equivalence ratio ϕ. The region of equivalence ratio $0.6 < \phi < 1.0$ is shown to produce high values of hydrogen

yield (≈70–80%) with realistic operating conditions (inlet velocity $U = 1\,\mathrm{m\,s^{-1}}$ and inlet temperature $T = 875\,\mathrm{K}$). Additionally, the operating temperature and the carbon soot on the catalyst surface are relative low resulting in favorable operational conditions.

The investigation is not based on a thermodynamic equilibrium analysis, but on the evaluation of the detailed surface mechanism. As a consequence, the residence time is the guiding parameter in the SPSR simulations. On the other hand, the predictions and the results presented herein are strongly influenced by the detailed surface chemistry mechanism employed. Future work aims at experiments that will further evaluate our conclusions.

An important conclusion of the present work is the effectiveness of the optimization concept based on a simple reactor configuration with low computational cost. Using the SPSR configuration it is possible to perform many simulations (of the order of thousands) in couple of hours on a standard 3.0 GHz Intel Xeon workstation. The parameter space can be extended to different monoliths, with different surface to volume ratio or catalyst coverage. Finally using different surface mechanisms the optimization can be extended to different fuels and catalysts.

Acknowledgments

Partial financial support for this work from Department of Energy of Switzerland (program manager Dr. A. Hintermann) is gratefully acknowledged. One of the authors (A.K.C.) is grateful to Dr. J. Mantzaras of the Combustion Fundamentals Group at Paul Scherrer Institute for helpful discussions.

References

[1] C.S. Song, Catal. Today 77 (2002) 17–49.
[2] D. zur Megede, J. Power Sources 106 (2002) 35–41.
[3] J.C. Mackie, Catal. Rev.-Sci. Eng. 33 (1991) 169–240.
[4] A. Docter, A. Lamm, J. Power Sources 84 (1999) 194–200.
[5] D.A. Hickman, L.D. Schmidt, Science 259 (1993) 343–346.
[6] D.A. Hickman, E.A. Haupfear, L.D. Schmidt, Catal. Lett. 17 (1993) 223–237.
[7] S.S. Bharadwaj, L.D. Schmidt, Fuel Process. Technol. 42 (1995) 109–127.
[8] F. Joensen, J.R. Rostrup-Nielsen, J. Power Sources 105 (2002) 195–201.
[9] D.A. Hickman, L.D. Schmidt, Aiche J. 39 (1993) 1164–1177.
[10] R.P. O'Connor, E.J. Klein, L.D. Schmidt, Catal. Lett. 70 (2000) 99–107.
[11] K.L. Hohn, L.D. Schmidt, Appl. Catal. A-Gen. 211 (2001) 53–68.
[12] L.D. Pfefferle, Catal. Today 26 (1995) 255–265.
[13] S.T. Kolaczkowski, Catal. Today 47 (1999) 209–218.
[14] R.S. Larson, Sandia Report SAND96-8211, 1996.
[15] L.C. Young, B.A. Finlayson, Aiche J. 22 (1976) 331–343.
[16] R.E. Hayes, S.T. Kolaczkowski, Chem. Eng. Sci. 49 (1994) 3587–3599.
[17] O. Deutschmann, L.D. Schmidt, Aiche J. 44 (1998) 2465–2477.
[18] C.T. Goralski, L.D. Schmidt, Chem. Eng. Sci. 54 (1999) 5791–5807.
[19] L.L. Raja, R.J. Kee, O. Deutschmann, J. Warnatz, L.D. Schmidt, Catal. Today 59 (2000) 47–60.
[20] H. Schlichting, K. Gersten, Boundary Layer Theory, Springer, Berlin, 2000.
[21] M.E. Coltrin, H.K. Moffat, R.J. Kee, F.M. Rupley, Sandia Report SAND93-0478, 1993.
[22] D.K. Zerkle, M.D. Allendorf, M. Wolf, O. Deutschmann, J. Catal. 196 (2000) 18–39.
[23] S. Tischer, C. Correa, O. Deutschmann, Catal. Today 69 (2001) 57–62.
[24] J. Mantzaras, C. Appel, Combust. Flame 130 (2002) 336–351.
[25] M. Reinke, J. Mantzaras, R. Schaeren, R. Bombach, A. Inauen, S. Schenker, Combust. Flame 136 (2004) 217–240.
[26] O. Deutschmann, R. Schwiedernoch, L.I. Maier, D. Chatterjee, in: E. Iglesia, J.J. Spivey, T.H. Fleisch (Eds.), Natural Gas Conversion VI, Studies in Surface Science and Catalysis, Elsevier, Amsterdam, 2001, pp. 215–258.
[27] S. Mazumder, D. Sengupta, Combust. Flame 131 (2002) 85–97.
[28] J.W. Geus, J.C. van Giezen, Catal. Today 47 (1999) 169–180.
[29] K. Maruta, K. Takeda, J. Ahn, K. Borer, L. Sitzki, et al., Proc. Combust. Inst. 29 (2003) 957–963.
[30] R. Schwiedernoch, S. Tischer, C. Correa, O. Deutschmann, Chem. Eng. Sci. 58 (2003) 633–642.
[31] R.B. Bird, W.E. Stewart, E.N. Lightfoot, Transport Phenomena, Wiley, New York, 1960.
[32] R.J. Kee, F.M. Rupley, E. Meeks, J.A. Miller, Sandia Report SAND96-8216, 1996.
[33] R.J. Kee, G. Dixon-Lewis, J. Warnatz, M.E. Coltrin, J.A. Miller, Sandia Report SAND86-8246, 1986.
[34] H.K. Moffat, R.J. Glarborg, R.J. Kee, J.F. Grcar, J.A. Miller, Sandia Report SAND91-8001, 1991.
[35] R.S. Sinkovits, C.R. DeVore, V.A. Shamamian, Diam. Relat. Mat. 5 (1996) 1344–1354.
[36] F. Moallemi, G. Batley, V. Dupont, T.J. Foster, M. Pourkashanian, A. Williams, Catal. Today 47 (1999) 235–244.
[37] S.H. Chan, H.M. Wang, Int. J. Hydrog. Energy 25 (2000) 441–449.
[38] S. Ahmed, M. Krumpelt, Int. J. Hydrog. Energy 26 (2001) 291–301.
[39] J. Zhu, D. Zhang, K.D. King, Fuel 80 (2001) 899–905.
[40] Y.S. Seo, A. Shirley, S.T. Kolaczkowski, J. Power Sources 108 (2002) 213–225.
[41] S.H. Chan, H.M. Wang, J. Power Sources 126 (2004) 8–15.
[42] B.F. Hagh, Int. J. Hydrog. Energy 28 (2003) 1369–1377.
[43] A. Ern, V. Giovangigli, M.D. Smooke, J. Comput. Phys. 126 (1996) 21–39.
[44] CFD-ACE+, Version 2004, ESI-CFD, Huntsville, AL, 20004.
[45] S. Mazumder, S.A. Lowry, J. Comput. Phys. 173 (2001) 512–526.
[46] O. Deutschmann, L.I. Maier, U. Riedel, A.H. Stroemman, R.W. Dibble, Catal. Today 59 (2000) 141–150.
[47] F.A. Williams, Combustion Theory; The Fundamental Theory of Chemically Reacting Flow Systems, Benjamin/Cummings Publishing Company, Menlo Park, 1985.
[48] T. Poinsot, D. Veynante, Theoretical and Numerical Combustion, R.T. Edwards, Inc., Philadelphia, PA, 2001.
[49] P. Canu, S. Vecchi, Aiche. J. 48 (2002) 2921–2935.
[50] K.K. Kuo, Principles of Combustion, John Wiley and Sons, New York, 1986.
[51] M.E. Coltrin, R.J. Kee, F.M. Rupley, Int. J. Chem. Kinet. 23 (1991) 1111–1128.